Molecular Cell
Article

A Direct HDAC4-MAP Kinase Crosstalk Activates Muscle Atrophy Program

Moon-Chang Choi,[1,4] Todd J. Cohen,[1,4] Tomasa Barrientos,[1] Bin Wang,[1] Ming Li,[1] Bryan J. Simmons,[1] Jeong Soo Yang,[2] Gregory A. Cox,[3] Yingming Zhao,[2] and Tso-Pang Yao[1,*]
[1]Department of Pharmacology and Cancer Biology, Duke University, Durham, NC 27710, USA
[2]The Ben May Department for Cancer Research, University of Chicago, Chicago, IL 60637, USA
[3]The Jackson Laboratory, 600 Main Street, Bar Harbor, ME 04609, USA
[4]These authors contributed equally to this work
*Correspondence: yao00001@mc.duke.edu
DOI 10.1016/j.molcel.2012.04.025

SUMMARY

Prolonged deficits in neural input activate pathological muscle remodeling, leading to atrophy. In denervated muscle, activation of the atrophy program requires HDAC4, a potent repressor of the master muscle transcription factor MEF2. However, the signaling mechanism that connects HDAC4, a protein deacetylase, to the atrophy machinery remains unknown. Here, we identify the AP1 transcription factor as a critical target of HDAC4 in neurogenic muscle atrophy. In denervated muscle, HDAC4 activates AP1-dependent transcription, whereas AP1 inactivation recapitulates HDAC4 deficiency and blunts the muscle atrophy program. We show that HDAC4 activates AP1 independently of its canonical transcriptional repressor activity. Surprisingly, HDAC4 stimulates AP1 activity by activating the MAP kinase cascade. We present evidence that HDAC4 binds and promotes the deacetylation and activation of a key MAP3 kinase, MEKK2. Our findings establish an HDAC4-MAPK-AP1 signaling axis essential for neurogenic muscle atrophy and uncover a direct crosstalk between acetylation- and phosphorylation-dependent signaling cascades.

INTRODUCTION

Adult skeletal muscle is a highly adaptive tissue that can undergo changes in size, contractility, and metabolism to meet functional demands. The plasticity of myofibers reflects coordinated changes in the muscle gene expression program controlled by neural activity (Bassel-Duby and Olson, 2006). While physiological remodeling confers adaptation, pathological remodeling caused by prolonged deficits in neural input can lead to muscle atrophy. In motor neuron diseases, such as amyotrophic lateral sclerosis (ALS), denervation-associated muscle atrophy is prevalent and contributes to breathing and moving difficulty and eventual death. While significant progress has been made in identifying downstream effectors in the muscle atrophy program including the ubiquitin E3 ligases, atrogin-1/MAFbx and MuRF1 (Bodine et al., 2001; Gomes et al., 2001), the signaling pathway that controls activity-dependent muscle atrophy remains poorly characterized. Such knowledge could provide insights into the development of therapeutic strategies for pathological muscle remodeling.

The protein deacetylase HDAC4 has emerged as a central component of muscle transcriptional reprogramming upon denervation. HDAC4 is robustly induced in surgically denervated muscle or in those affected by motor neuron diseases such as ALS (Cohen et al., 2007). In denervated muscle, elevated HDAC4 has a dual role: it represses muscle structural gene transcription (Cohen et al., 2009) but also induces genes involved in synapse formation and muscle atrophy (Cohen et al., 2007; Moresi et al., 2010; Tang et al., 2009). We previously showed that HDAC4 represses the Dach2 transcription repressor, resulting in the induction of the myogenin transcription factor and synaptic gene transcription (Cohen et al., 2007). Interestingly, the HDAC4-Dach2-myogenin transcriptional axis is also required for full induction of the ubiquitin E3 ligases MuRF1 and atrogin-1 that promote atrophy (Cohen et al., 2007; Macpherson et al., 2011; Moresi et al., 2010). Mechanistically, HDAC4 has been extensively characterized as a classical transcriptional corepressor that binds and potently inhibits the master muscle transcription factor MEF2 (McKinsey et al., 2000). Paradoxically, however, the conserved histone deacetylase domain of HDAC4 is completely dispensable for this activity (Chan et al., 2003). This finding suggests a yet to be characterized mode of deacetylase-dependent activity for HDAC4. In this context, while MEF2 is the canonical target of HDAC4 in muscle structural gene transcription (Cohen et al., 2009), how HDAC4 is connected to the muscle atrophy program remains unclear.

In this study, we show that HDAC4 activates neurogenic muscle atrophy independent of its canonical transcriptional repressor activity toward MEF2. Instead, denervation-induced HDAC4 activates the AP1 transcription factor by stimulating MAP kinase signaling. Unlike its intrinsic transcriptional repressor activity, we found that a functional deacetylase domain is obligatory for HDAC4 to activate the MAPK-AP1 axis. We show that HDAC4 binds and promotes deacetylation of a MAP3K2, MEKK2, thereby promoting MAPK-AP1 signaling and muscle atrophy. Our study identifies an HDAC4-MAP kinase-AP1 network as the critical effector in denervation-induced

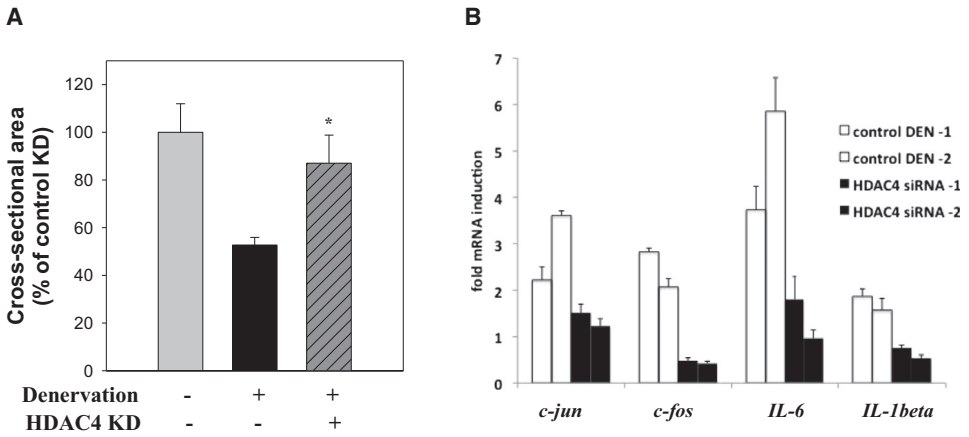

Figure 1. HDAC4 Is Required for Denervation-Induced Muscle Atrophy and AP1-Cytokines Expression

(A) Quantification of mean fiber CSA (cross-sectional area) in TA muscle of control KD, control KD-denervated, and HDAC4 KD-denervated mice 14 days after denervation. Values are expressed as percentage of control KD. Columns, mean; bars, SEM n = 3 for each group. *p < 0.05 versus control KD denervated (unpaired Student's t test).

(B) Expressions of inflammatory cytokines and AP1 in denervated muscle mediated by HDAC4. The fold induction of *c-jun*, *c-fos*, *IL-6*, and *IL-1beta* mRNA 14 days after denervation was determined in control or HDAC4-siRNA transfected TA muscle by real-time RT-PCR. Values were normalized to actin. Error bars were generated from real-time PCR triplicates and represent SD (n = 2 per group). See Figure S1.

atrophy and uncovers a direct crosstalk between HDAC and MAP kinase signaling.

RESULTS

The AP1-Cytokine Transcriptional Network Is Activated by HDAC4 in Denervated Muscle

To unravel the mechanism by which HDAC4 promotes atrophy, we performed gene expression analysis to identify potential transcriptional targets of HDAC4 in denervated muscle. Mouse tibialis anterior (TA) muscles were transfected with control siRNA or HDAC4-specific siRNA by electroporation followed by surgical denervation for 14 days, and then subjected to morphometric or gene expression analysis. Introduction of HDAC4-specific siRNA significantly inhibited denervation-induced atrophy (Figure 1A) as was also shown previously (Moresi et al., 2010). Analysis of HDAC4 knockdown (KD) and control denervated muscles revealed the induction of many inflammatory cytokines in denervated muscle in an HDAC4-dependent manner (Figure S1A available online). Direct real-time RT-PCR analysis confirmed the induction of representative cytokines, *IL-6* and *IL-1beta*, in control but not HDAC4 KD denervated muscles (Figure 1B). Gene expression analysis also revealed the induction of *c-jun* and *c-fos*, key components of the AP1 transcription factor that activates inflammatory cytokine gene transcription (Adcock, 1997). Immunostaining analysis confirmed a prominent accumulation of c-*jun* in denervated muscle but the induction was lost upon KD of HDAC4 (Figure S1B). These results identify the AP1-inflammatory cytokine transcriptional program as a regulatory target of HDAC4 in denervated muscle.

Since inflammatory cytokine production has been implicated in the activation of the muscle atrophy program associated with cancer cachexia (Argilés et al., 2003; Bossola et al., 2008; Späte and Schulze, 2004), we reasoned that the AP1-dependent cytokine transcription program might be important in denervation-induced atrophy. To test this possibility, we inactivated AP1 in skeletal muscle by introducing a specific c-*fos* siRNA into TA muscle. As shown in Figure 2A, knockdown of c-*fos* effectively blunted the induction of *IL-6* and *IL-1beta* in denervated TA muscles, indicating that AP1 activates inflammatory cytokine transcription in response to denervation. Most importantly, myofibers receiving c-*fos* siRNA were also much more resistant to atrophy induced by denervation (Figure 2B). Consistent with this finding, the inductions of *MuRF1* and *atrogin-1* were markedly suppressed by c-*fos* KD (Figure 2C). Similarly, KD of c-*jun* also curbed the induction of ubiquitin E3 ligases (Figure S2). Interestingly, c-*fos* KD had no significant effect on *myogenin* expression (Figure 2C), indicating that AP1 regulates atrophy independent of myogenin induction. Together, these results demonstrate that HDAC4-dependent AP1 activity is a critical component of denervation-induced cytokine production and muscle atrophy.

HDAC4 Stimulates AP1 Activity by Activating the MAP Kinase-Signaling Cascade

We next determined how HDAC4 regulates the AP1 transcription network. To recapitulate the elevated levels of HDAC4 in denervated muscle, we transfected C2C12 myoblasts with an HDAC4 expression plasmid and analyzed AP1 activity using a reporter assay. In stark contrast to its robust inhibitory activity on a MEF2 reporter, HDAC4 potently activated the AP1 reporter (>10-fold, Figure 3A). Interestingly, HDAC5 and other class IIA HDAC members, which are also known to inhibit MEF2 (Haberland et al., 2009), did not activate the AP1 reporter (Figure S3). These results suggest that HDAC4 regulates AP1 and MEF2 activity by distinct mechanisms. Supporting this possibility, we found that the nuclear-localized HDAC4 3SA mutant, which encodes a super repressor of MEF2 (Zhao et al., 2001), was also ineffective for full activation of AP1. Importantly, while the

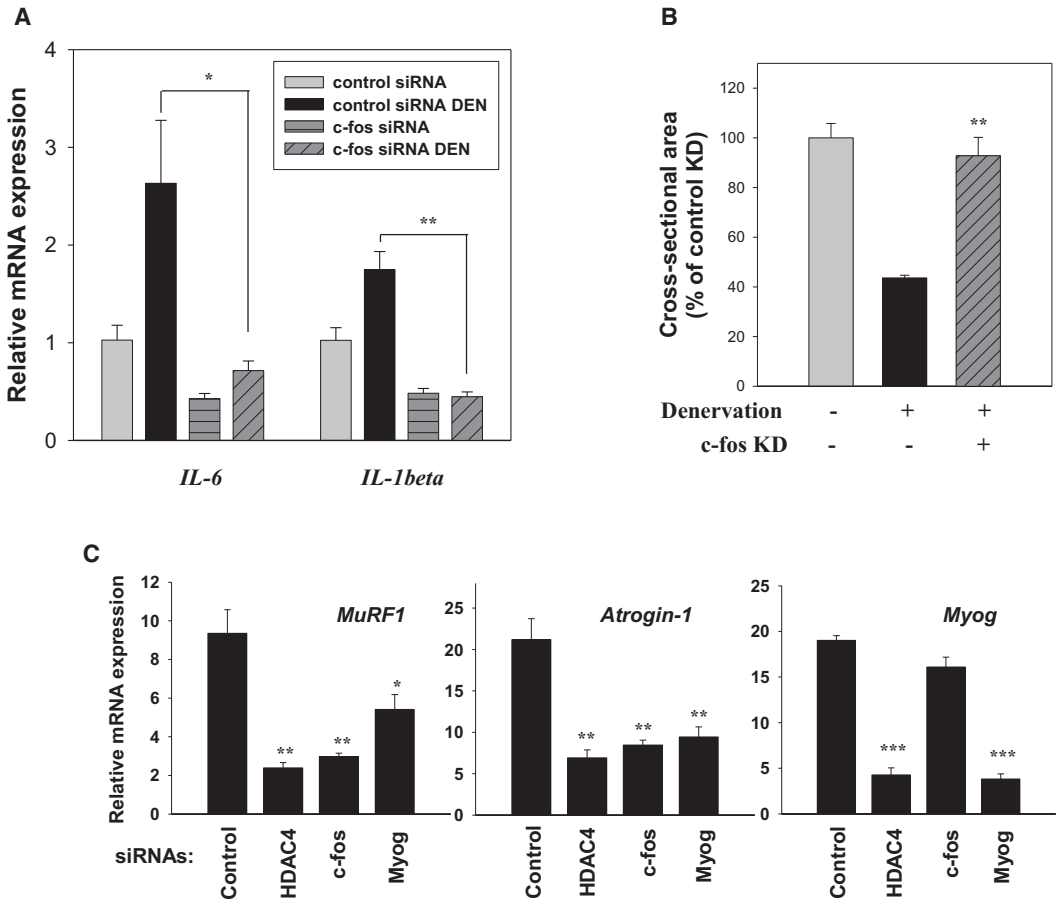

Figure 2. The AP1 Transcription Factor Regulated by HDAC4 Is Critical for Denervation-Induced Muscle Atrophy and Cytokine Expression

(A) Expressions of *IL-6* and *IL-1beta* were detected by real-time RT-PCR in TA muscle electroporated with control or c-fos siRNA and denervated for 14 days. Values were normalized to actin. Columns, mean (n = 3 for each group); bars, SEM. *p < 0.05, **p < 0.01 versus control siRNA DEN (unpaired Student's t test).

(B) Mean fiber CSA was quantified to determine fiber size in TA muscle of control KD, control KD-denervated, and c-fos KD-denervated mice 14 days after denervation. Values are expressed as percentage of control KD. Columns, mean; bars, SEM n = 3 for each group. **p < 0.01 versus control KD denervated (unpaired Student's t test).

(C) Expressions of MuRF1, atrogin-1, and myogenin were determined by real-time RT-PCR in TA muscles that were electroporated with control, HDAC4, c-fos or myogenin siRNA and denervated for 7 days. Values were normalized to GAPDH. Relative fold change was calculated compared to control siRNA non-DEN. Columns, mean; bars, SEM n = 4 for each group. *p < 0.05, **p < 0.01, ***p < 0.001 versus control siRNA DEN (unpaired Student's t test). See Figure S2.

catalytic activity of HDAC4 is completely dispensable for repressing MEF2 activity (Chan et al., 2003), the catalytically deficient HDAC4 (CAD) mutant failed to activate the AP1 reporter. Together, these results show that HDAC4 activates AP1 activity independent of its well-characterized transcriptional repressor activity but requires an intact catalytic domain.

AP1 induction and activation are regulated by the MAP kinases including Erk1/2, p38, and JNK (Eferl and Wagner, 2003). We next considered the possibility that HDAC4 might regulate AP1 by intersecting with the MAP kinase-signaling pathway. To this end, we used pharmacological inhibitors or dominant-negative (DN) mutants to selectively inhibit each of the three main MAP kinases, Erk, p38, and JNK. As shown in Figures 3B and 3C, we found that inhibition of the MEK-Erk pathway by an MEK1/2 inhibitor U0126 or DN-MEK1 potently repressed AP1 activity induced by HDAC4, while the p38 kinase inhibitor SB202190 or DN-MKK6 had a more moderate effect. In contrast, inhibition of JNK by SP600125 or DN-JNK1 had little effect (Figures 3B and 3C). Supporting these observations, combined treatment of MEK1/2 and p38 but not JNK inhibitors completely abolished HDAC4-induced AP1 activity (Figure 3B, last two columns). These results show that HDAC4-dependent AP1 activity requires active MEK1/2-Erk1/2 and MKK3/6-p38 MAPK signaling.

We next asked if elevated levels of HDAC4 could activate the MEK-Erk or MKK3/6-p38 kinase pathways. Using antibodies for the phosphorylated and activated form of the kinases, we found that overexpression of HDAC4 led to an increase in phospho-MEK1/2 and -Erk1/2 (Figure 4A) as well as phospho-p38 (Figures 4B and S4A) and -MKK3 (Figure S4B) indicating that both MAPK pathways were activated. Supporting this conclusion, overexpression of HDAC4 induced c-*fos* Thr-325 phosphorylation (Figure 4C), which is a known target of Erk1/2 and is associated with AP1 activation (Assoian, 2002). HDAC4-CAD or 3SA mutants, which cannot activate AP1, also failed to promote MAPK

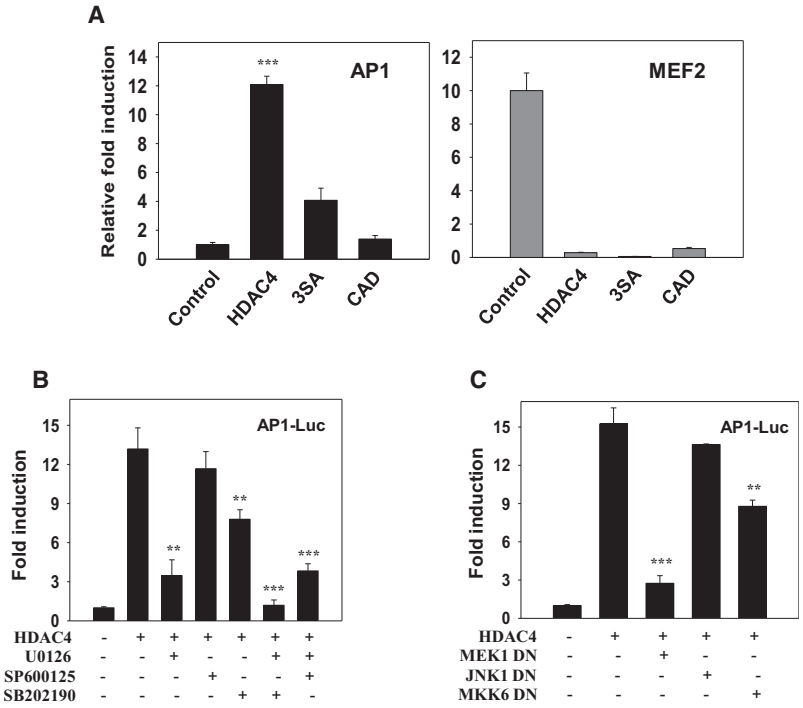

Figure 3. HDAC4 Activates AP1 by a MAPK-Dependent but MEF2-Independent Mechanism

(A) AP1 activation by HDAC4. AP1 (left panel) or MEF2 reporter (right panel) activity was measured in C2C12 myoblasts transfected with an expression plasmid of HDAC4 WT, nuclear localized mutant (3SA), or catalytically dead mutant (CAD, histidines 802 and 803 replaced with lysine and leucine, respectively). Columns, mean; Bars, SD (n = 3). ***p < 0.001 versus control.

(B) C2C12 cells were cotransfected with HDAC4 and an AP1 reporter and subsequently treated with inhibitors for MEK1/2 (U0126, 10 μM), JNK (SP600125, 10 μM), p38 (SB202190, 20 μM). Lysates were then subjected to the luciferase reporter assay. Columns, mean; Bars, SD (n = 3). **p < 0.01, ***p < 0.001 versus HDAC4 overexpression with no treatment.

(C) Effect of dominant-negative (DN) mutants against MAP kinase pathway on HDAC4-induced AP1 activation. Columns, mean; Bars, SD (n = 3). ***p < 0.001 versus HDAC4 overexpression. See Figure S3.

phosphorylation (Figures 4A and 4B). Collectively, these results indicate that elevated levels of HDAC4 activate MAPK signaling which in turn stimulates AP1 activity.

MEKK2 Is Required for HDAC4 to Activate the MAPK-AP1 Signaling Cascade

The activation of MAP2Ks, including MEK1, often requires upstream kinases, MAP3Ks. There are at least 14 MAP3 kinases identified in mammalian cells (Zhang and Dong, 2005). Among MAP3 kinases, the Raf kinases are best characterized. However, pharmacological inhibition of B-Raf and C-Raf kinase had no effect on AP1 or MEK1 activation induced by HDAC4 (Figures S5A and S5B). Screening through additional MAP3K members by siRNA identified MEKK2 as a potential mediator of HDAC4 (Figure S5C). Indeed, inhibition of MEKK2 but not MEKK1, by siRNA or a dominant-negative mutant markedly suppressed HDAC4-induced AP1 and MEK1 activation (Figures 5A, 5B, and S5D). Interestingly, additional inactivation of MEKK4, a MAP3K required for MKK3-p38 signaling (Abell et al., 2007) (Figure S5E) further inhibited HDAC4-induced AP1 activation (Figure 5C). Together, these results indicate that HDAC4 activates AP1 via the MAPK pathway, primarily by a MEKK2-dependent mechanism.

HDAC4 Binds and Promotes MEKK2 Deacetylation

We next determined how HDAC4 is connected with MEKK2. Since an intact HDAC4 catalytic domain is required for AP1 activation (Figure 3A), we investigated if MEKK2 is subject to acetylation. We found that MEKK2 becomes acetylated upon coexpression with the acetyltransferases CREB-binding protein (CBP) (Figure 6A) or P/CAF (Figure S6A). Further, MEKK2 forms a complex with HDAC4 (Figure 6B) and becomes partially deacetylated when incubated with immunoprecipitated HDAC4 (Figure 6C). Importantly, endogenous MEKK2 purified from normal TA muscles is also subject to acetylation, and this acetylation is largely lost upon denervation (Figure 6D). Supporting an important role of HDAC4 in denervation-induced MEKK2 deacetylation, knockdown of HDAC4 significantly restored MEKK2 acetylation in denervated muscles (Figures 6D and 6E). These results show that HDAC4 can bind and promote MEKK2 deacetylation.

To investigate the role of MEKK2 acetylation, we determined the acetylation sites in MEKK2 by mass spectrometry. Interestingly, the three lysine residues acetylated by both CBP and P/CAF are all localized to the catalytic domain (Table S1). Among them, Lys385 is a conserved residue required for kinase activity (Chayama et al., 2001; Fanger et al., 1997). Mutation of Lys(K)385 to methionine (MEKK2-K385M) reduced CBP-mediated MEKK2 acetylation, confirming that K385 is subject to acetylation (Figure 6F). Supporting these observations, MEKK2 purified from cells overexpressing CBP had lower kinase activity than MEKK2 from control cells (Figure S6B). To further assess if acetylation affects MEKK2 activity, we generated an acetylation-mimicking K385Q (glutamine) mutant MEKK2. We found that K385Q-MEKK2 is deficient in kinase activity (Figure 6G) and AP1 activation (Figure S6C). These results indicate that acetylation inhibits MEKK2 activity and HDAC4 activates MEKK2 activity by stimulating its deacetylation.

HDAC4-Dependent MAPK Signaling Is Required for Denervation-Induced Muscle Atrophy

To determine if the HDAC4-MAPK-AP1 signaling cascade is indeed involved in denervation-induced atrophy, we assessed the MAPK signaling status in denervated muscle. Upon denervation, MEK1/2 and Erk phosphorylation, and c-*jun* and c-*fos* induction were observed (Figure 7A). Similarly, phospho-MEK1/2, phospho-Erk1/2, and c-*jun* were induced in muscles from an ALS mouse model (SOD1-G93A) suffering from denervation

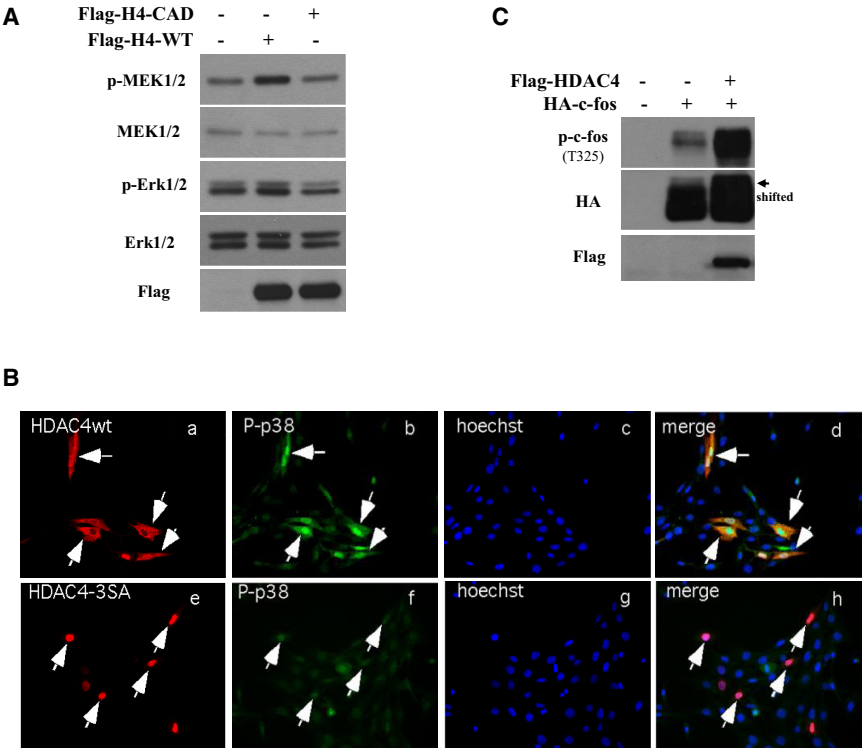

Figure 4. Activation of MAP Kinase Signaling by HDAC4

(A) Flag-tagged HDAC4 wild-type (WT) or catalytically dead mutant (CAD) was transfected into C2C12 myoblasts with equal amount of expression, and lysates were subjected to western blotting using p-MEK1/2 and p-Erk1/2 antibodies.

(B) Activation of endogenous p38 by HDAC4. Cells were transfected with Flag-HDAC4 and stained with anti-Flag antibody (red) and anti-phospho-p38 antibody (green). DNA (blue) was visualized by Hoechst staining.

(C) Flag-tagged HDAC4 was cotransfected into C2C12 myoblasts with HA-c-*fos*, and activation of c-*fos* was detected using p-c-*fos* (Thr325) antibody. See Figure S4.

and atrophy (Figure S7A). Importantly, denervation-induced MEK-Erk activation (Figure 7B) and AP1 induction (Figure 7C) were markedly inhibited in muscles expressing an HDAC4-siRNA, further supporting the notion that HDAC4 activates the MAPK-AP1 signaling cascade in response to denervation. Interestingly, MEKK2 accumulation was observed in denervated muscles (Figure 7A), which depends on HDAC4 (Figure 7B), as well as in ALS-affected muscles (Figure S7A). To determine if MEKK2 is required for muscle atrophy, we electroporated MEKK2-specific siRNA into TA muscles. As shown in Figures 7D, 7E, and S7B, MEKK2 knockdown attenuated muscle atrophy (Figures 7D and S7B) and the expression of *MuRF1* and *atrogin-1* induced by denervation (Figure 7E). The significant but partial effect of MEKK2 KD on muscle atrophy likely reflects the involvement of an additional MAP3 kinase, MEKK4 (Figures 5C and S5E). Future studies using MEKK2 and MEKK4 knockout mice would be needed to confirm their specific contribution to muscle atrophy (Guo et al., 2002). Collectively, these results demonstrate that HDAC4, the MAP kinase cascade, and the AP1 transcription factor constitute a key signaling pathway that executes the muscle atrophy program induced by loss of neural inputs.

DISCUSSION

In this report, we provide evidence that HDAC4 promotes neurogenic muscle atrophy, at least in part, by activating the MAPK-AP1 signaling cascade. c-*jun* and c-*fos*, the two major AP1 subunits, have long been known to be induced in denervated muscle but with no known significance (Weis, 1994). Our finding that inactivation of c-*fos* significantly blunted the muscle atrophy program identifies AP1 as a critical component in the execution of neurogenic muscle atrophy (Figures 2B and 2C). Interestingly, AP1 and inflammatory cytokines have been implicated in atrophy associated with cancer cachexia (Argilés et al., 2003; Moore-Carrasco et al., 2006, 2007). We suspect that AP1-dependent cytokine production might collectively contribute to pathological muscle remodeling in denervated muscle. Future experiments would be required to determine whether the HDAC4-AP1-cytokine axis is similarly involved in cancer cachexia.

Myogenin, which is transcriptionally induced upon denervation by an HDAC4-dependent mechanism (Cohen et al., 2007), was recently reported to activate *MuRF1* and *atrogin-1* transcription and muscle atrophy (Moresi et al., 2010). Interestingly, we found that AP1 inactivation blunted the induction of *MuRF1* and *atrogin-1* in denervated muscle but had little effect on *myogenin* expression (Figure 2C). These findings reveal that HDAC4 regulates muscle atrophy by two independent pathways that converge on MuRF1 and atrogin-1 transcription. This arrangement might allow for a more efficient regulation of muscle mass in response to changes in neural and muscle activity. Importantly, our results indicate that HDAC4 activates the MAPK-AP1 signaling cascade independent of its canonical transcription repressor activity but requires an intact catalytic domain. It has long been recognized that the transcriptional repressor activity of HDAC4 does not require its catalytic domain (Zhao et al., 2005). Accordingly, any specific function of the conserved catalytic domain has been elusive. In fact, evidence indicates that HDAC4 and related class IIA HDAC members do not encode for classical histone deacetylases (Bottomley et al., 2008; Fischle et al., 2002; Lahm et al., 2007). It is generally thought that HDAC4 promotes deacetylation by recruiting HDAC3 (Fischle et al., 2002; Zhao et al., 2005). However, we found that HDAC3 does not activate AP1 (Figure S3) and is not required for HDAC4 to activate AP1 (data not shown). While the detailed mechanism by which HDAC4 facilitates MEKK2 deacetylation remains to be determined, the distinct mechanisms

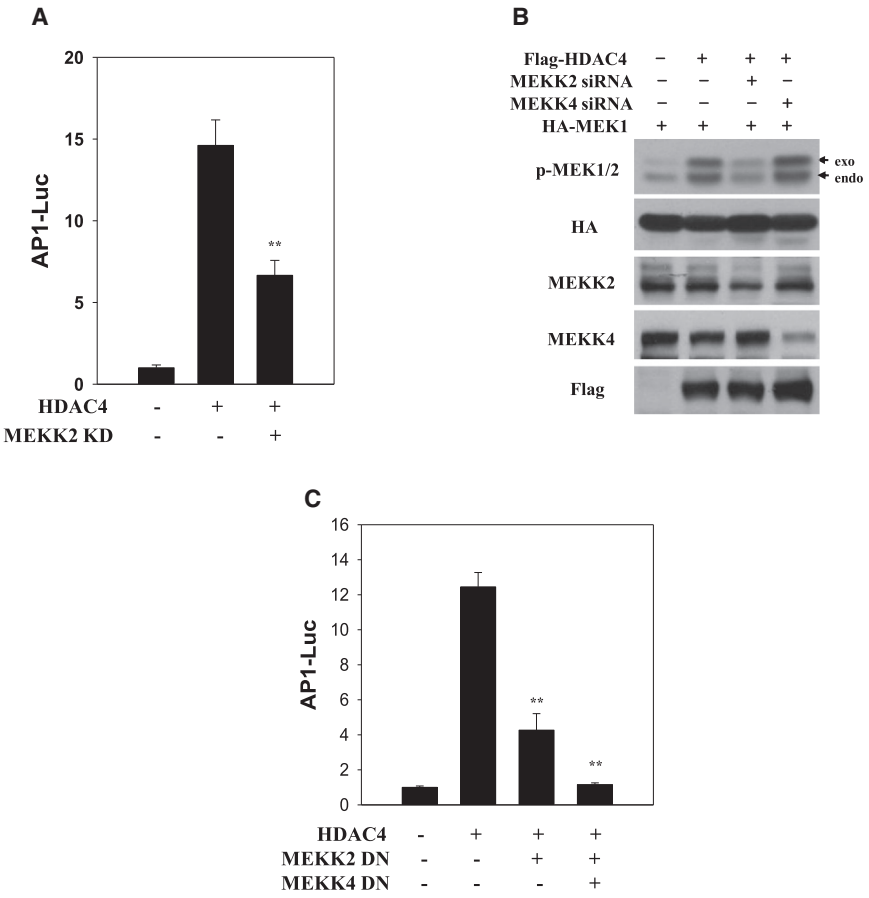

Figure 5. MEKK2 Is Required for HDAC4 to Activate AP1 and MEK1

(A) The inhibition of AP1 activity by MEKK2 KD in HDAC4-overexpressing cells. Columns, mean; Bars, SD (n = 3). **p < 0.01 versus HDAC4 overexpression.

(B) Effect of MEKK2 KD on MEK1 activation induced by HDAC4. Activation of MEK1 was determined by immunoblotting with the phospho-MEK1/2 antibody.

(C) Suppression of AP1 activity by double inhibition of MEKK2 and MEKK4 in HDAC4-overexpressing C2C12 cells. MEKK2 and MEKK4 were inhibited by transfecting dominant-negative (DN) mutants in C2C12 myoblasts, and AP1 activity induced by HDAC4 was measured by luciferase assay. Columns, mean; Bars, SD (n = 3). **p < 0.01 versus HDAC4 overexpression. See Figure S5.

used by HDAC4 to regulate MEF2 and the MAPK-AP1 axis highlights a potential strategy to selectively inhibit HDAC4 activity without affecting critical MEF2-dependent transcriptional programs. Such a possibility provides a rationale for selectively targeting HDAC4 catalytic domain-dependent activity in neuromuscular diseases and other related disorders.

Our data indicate that HDAC4 activates MAPK signaling, at least in part, by binding and promoting MEKK2 deacetylation. Interestingly, a bacterial acetyltransferase, VopA, was previously shown to acetylate the ATP-binding lysine residues and inactivate MKK6 kinase, thereby inhibiting MAPK signaling and host innate immune response (Trosky et al., 2007). Collectively, these findings suggest that MAP kinase acetylation is an endogenous cellular regulatory mechanism, which is hijacked by the pathogen to gain control of MAPK-dependent innate immunity. The direct HDAC4-MAP kinase crosstalk uncovered in this study not only would greatly amplify the regulatory power of protein acetylation but also expand the potential clinical applications of HDAC inhibitors in the future.

EXPERIMENTAL PROCEDURES

Cell Culture/Plasmids/Antibodies

C2C12 myoblasts and 293T cells were cultured in 20% FBS/DMEM and 10% FBS/DMEM, respectively. Cells were maintained at 37°C in a humidified atmosphere with 5% CO_2.

The HDAC4-3SA expression plasmid was generated by subcloning the coding sequence from PBJ-HDAC4-3SA into the pcDNA3 vector. Flag-HDAC4-CAD (histidines 802 and 803 replaced with lysine and leucine, respectively) and HA-MEKK2-K385Q were generated by the standard protocol for PCR-mediated mutagenesis, and the constructs were confirmed by DNA sequencing. The following plasmids have been described previously: Flag-HDAC4-WT (Zhao et al., 2005), Flag-HDAC5 (Zhao et al., 2005), HA-MEK1-8E (K97M) (Mansour et al., 1994), JNK1-APF (Ke et al., 2010), MKK6-K82M (Yuasa et al., 1998), HA-MEK1-WT (Mansour et al., 1994), HA-Erk1 (from J. Kyriakis), HA-c-*fos* (Morimoto et al., 2007), HA-MKK3 (Molnár et al., 1997), HA-p38 (from J. Kyriakis), HA-MEKK2 (Blank et al., 1996), myc-MEKK2 (Blonska et al., 2004), HA-CBP-WT (Zhao et al., 2005), HA-CBP-CAD (LD) (Zhao et al., 2005), MEKK1-K1253M (Widmann et al., 1998), HA-MEKK2-K385M (Fanger et al., 1997), HA-MEKK4-K1361M (Gerwins et al., 1997), AP1-Luc (Ke et al., 2010), and MEF2-Luc (Zhao et al., 2001).

The following antibodies were used: p-MEK1/2, total MEK1/2, p-Erk1/2, total Erk1/2, p-p38, p-MKK3/6, pan Acetyl-K, and glyceraldehyde-3-phosphate dehydrogenase (GAPDH) antibodies from Cell Signaling; c-*jun*, c-*fos*, and MEKK4 antibodies from Santa Cruz; p-c-*fos* antibody from Invitrogen; MEKK2 antibody from Abcam and Santa Cruz; Flag and HA antibodies from Sigma; and myc antibody from Covance. Polyclonal anti-HDAC4 antibody was previously described (Zhao et al., 2001).

Mouse Procedures

All mice used for electroporation and denervation were on the C57BL/6 background and were 6–8 weeks old (Jackson Laboratories). SOD1-G93A transgenic mice were also purchased from Jackson Laboratories. Stealth siRNA duplexed oligos were from Invitrogen.

For in vivo electroporation analysis, control siRNA or siRNA specific for HDAC4, c-*fos*, myogenin, c-*jun*, or MEKK2 were injected into TA muscles with a green fluorescent protein (GFP) plasmid included to identify electroporated fibers as described previously (Cohen et al., 2009). Mice were anesthetized with a ketamine/xylazine mixture, and siRNA was directly injected into TA muscles using a cemented MicroSyringe (Hamilton). An ECM830 electroporator (BTX) was used for all electroporations. The efficacy of siRNAs was confirmed in cells or muscles. The following siRNA sequences were used in mice or cells: HDAC4, 5′-GAGCAGCAGAGGAUCCACCAGUUAA-3′; three pooled c-*fos* siRNAs, 5′-CCGGGCUGCACUACUUACACGUCUU-3′, 5′-UCU

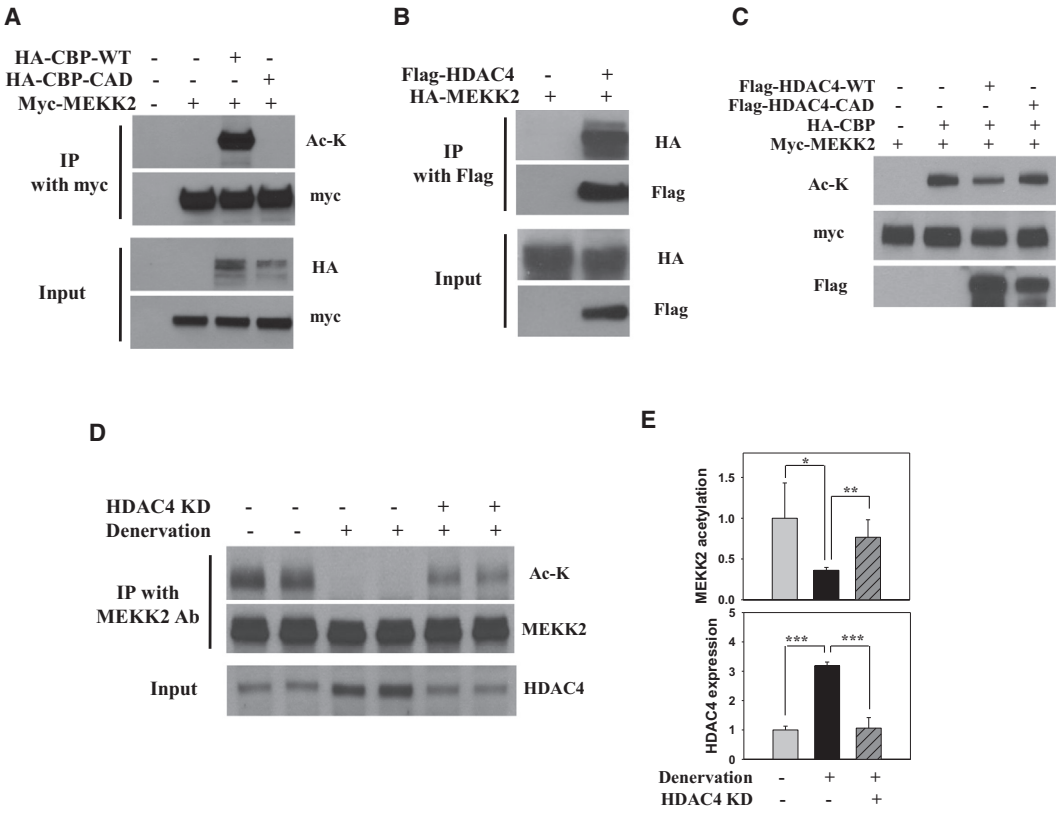

Figure 6. MEKK2 Is Subject to Reversible Acetylation, and HDAC4 Promotes MEKK2 Deacetylation

(A) Detection of acetylated MEKK2 induced by CBP. Myc-tagged MEKK2 was cotransfected with CBP WT or catalytic-inactive mutant (CAD) into 293T cells. Immunoprecipitated MEKK2 was then subject to immunoblotting with an antibody for acetylated lysine (Ac-K).

(B) HDAC4 interacts with MEKK2. 293T cells were cotransfected with Flag-HDAC4 and HA-MEKK2. Cell lysates were immunoprecipitated and immunoblotted with the indicated antibodies.

(C) Deacetylation of MEKK2 by purified HDAC4 WT but not by HDAC4 CAD mutant.

(D) Deacetylation of MEKK2 by HDAC4 in denervated muscle for 3 days.

(E) Quantification of MEKK2 acetylation and HDAC4 expression from independent western blot experiments. MEKK2 acetylation and HDAC4 expression were normalized to total MEKK2 and to GAPDH expression, respectively. Columns, mean; Bars, SD ($n = 4$). *$p < 0.05$, **$p < 0.01$, ***$p < 0.001$ (unpaired Student's t test).

(F) Reduction of acetylated MEKK2 levels in MEKK2-K385M construct mutated at Lys385, a residue required for ATP binding and MEKK2 kinase activity.

(G) The effect of MEKK2 acetylation on kinase activity. Proteins coding MEKK2 WT or K385Q were incubated with a substrate, HA-MEK1-K97M. Kinase activity was assessed by immunoblotting with p-MEK1/2 antibody. See Figure S6.

GUCCGUCUCUAGUGCCAACUUU-3′, and 5′-GGCUGCACUACUUACACGU CUUCCU-3′; three pooled myogenin siRNAs, 5′-GGGAGAAGCGCAGGCU CAAGAAAGU-3′, 5′-CCUUGCUCAGCUCCCUCAACCAGGA-3′, and 5′-CAG ACGCCCACAAUCUGCACUCCCU-3′; three pooled c-*jun* siRNAs, 5′-GAG AGCGGUGCCUACGGCUACAGUA-3′, 5′-UGGCACAGCUUAAGCAGAAAGU CAU-3′ and GCUAACGCAGCAGUUGCAAACGUUU-3′; MEKK2, 5′-GGGCA CAGAGCUACCCAGAUAAUCA-3′; MEKK4, 5′-UACACUUCUGCUCUGAGGA AGGAGG-3′.

For surgical denervation experiment, mice were anesthetized, the sciatic nerve was exposed, and an ~5 mm piece was excised as described

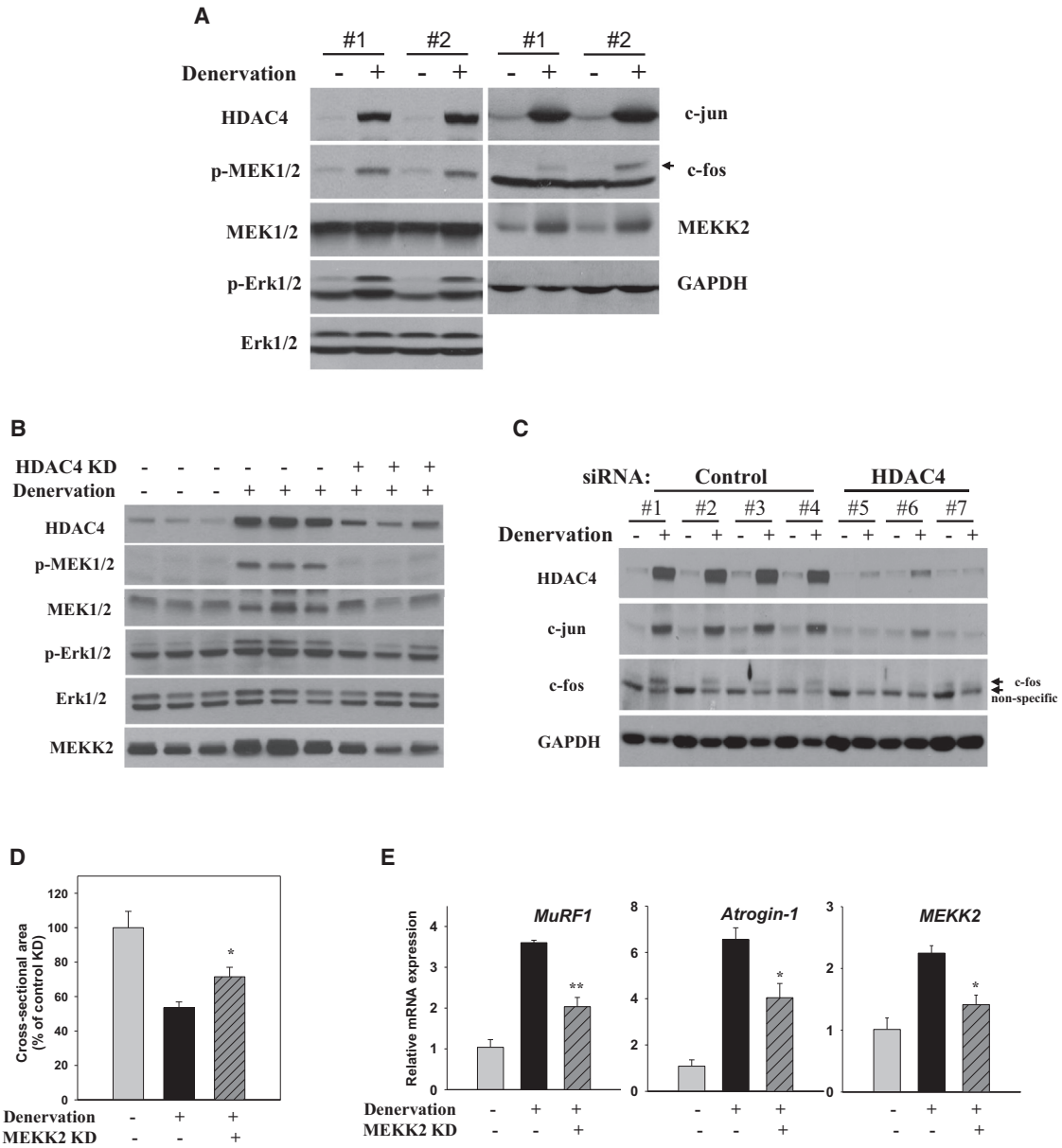

Figure 7. The MAPK Signaling Cascade Is Activated in Denervated Muscle and Is Required for Proper Execution of Neurogenic Muscle Atrophy

(A) Activation of the HDAC4-MAPK-AP1 axis during denervation. Innervated and 4 day denervated muscles were immunoblotted for MAPK components with the indicated antibodies.

(B) Inhibition of MAPK signaling by HDAC4 KD in denervated muscle. Western blot analysis was performed using lysates from TA muscles electroporated with control or an HDAC4-specific siRNA followed by 5 days of denervation.

(C) HDAC4-dependent AP1 induction in denervated muscles for 7 days.

(D) Quantification of mean fiber CSA in TA muscle of control KD, control KD-denervated, and MEKK2 KD-denervated mice 7 days after denervation. Values are expressed as percentage of control KD. Columns, mean; bars, SEM n = 3 for each group. *p < 0.05 versus control KD-denervated (unpaired Student's t test).

(E) Effect of MEKK2 KD on the expressions of ubiquitin E3 ligases. Expressions of *MuRF1*, *atrogin-1*, and *MEKK2* were determined by real-time RT-PCR in TA muscles that were electroporated with control or MEKK2 siRNA and denervated for 10 days. Values were normalized to GAPDH. Columns, mean; bars, SEM n = 3 for each group. *p < 0.05, **p < 0.01 versus control siRNA DEN (unpaired Student's t test). See Figure S7.

previously (Cohen et al., 2007). Denervation was confirmed by the loss of nerves when muscles were isolated. Mice were sacrificed by CO_2 euthanasia. All mice were housed at the Duke University mouse facilities in accordance with the Institutional Animal Care and Use Committee.

Immunostaining and Morphometric Analysis

Cells transfected by Flag-HDAC4-WT or Flag-HDAC4-3SA were fixed in 3.7% formaldehyde in PBS and then permeabilized with 0.1% Triton X-100 in PBS for 5 min at room temperature. Cells were blocked with 5% normal goat serum

in PBS and incubated with anti-p-p38 antibody, followed by Alexa Fluor 488 goat anti-rabbit IgG. HDAC4 was detected by subsequent staining using anti-Flag antibody. Nuclei were identified using Hoechst dye. Immunofluorescence images were obtained using a Zeiss Axioskop compound microscope (Carl Zeiss).

Muscle staining was performed as described previously (Cohen et al., 2009). TA muscles were frozen in methylbutane chilled in liquid nitrogen. Cryosections were stained with dystrophin antibody (NCL-DYS1) to mark muscle fibers and GFP antibody to identify the transfected fibers. The cross-sectional area of approximately 200 GFP-positive muscle fibers was quantified using ImageJ software (NIH). Values were plotted and expressed as percent of fibers at a given cross-sectional area.

Luciferase Assay

The luciferase reporter assay was performed as described previously (Cohen et al., 2009). Briefly, C2C12 cells were plated at 1,500 cells/well in a 24-well plate. Each AP1 or MEF2 reporter was cotransfected with renilla reporter in combination with the plasmids by using Lipofectamine LTX and Plus reagent (Invitrogen). Cells were lysed with passive lysis buffer (Promega) at 36–48 hr posttransfection unless otherwise mentioned, and luciferase assays were performed using the dual luciferase reporter assay kit (Promega). Each experiment was performed in triplicate. For pharmacological inhibition, at 16 hr posttransfection cells were treated with the inhibitors for additional 12 hr at a concentration indicated in the figure legends.

Gene Expression and RNA Analysis

RNA extraction and real-time RT-PCR were performed as described previously (Cohen et al., 2007). Superarray analysis was performed with samples obtained from TA muscles according to manufacturer's protocol (SABiosciences). TA muscles were dounce homogenized in TRIzol reagent (Invitrogen) on ice and RNA was isolated by a standard method. cDNA synthesis was carried out with oligo dT primer and an Improm II reverse transcription system (Promega) according to manufacturer's instructions. Real-time RT-PCR was performed using iQ SYBR supermix on the iCycler iQ detection system (Bio-Rad). All values were normalized to either actin or GAPDH and were expressed as fold changes versus levels measured in control samples. RT-PCR primer sequences were as follows: MuRF1, 5′-AGGTGAAGGAGGAGCTGAGTC-3′ and 5′-CATGTTCTCAAAGCCTTGCTC-3′; atrogin-1, 5′-TATGCACACTGGTG CAGAGAG-3′ and 5′-GTTGTCGTGTGCTGGGATTAT-3′; myogenin, 5′-GCAG GCTCAAGAAAGTGAATG-3′ and 5′-CACTTAAAAGCCCCCTGCTAC-3′; c-*jun*, 5′-CGCACAGCCCAGGCTAAC-3′ and 5′-TGAGGGCATCGTCGTAGAA-3′; c-*fos*, 5′-AGAGCGGGAATGGTGAAG-3′ and 5′-GGATTCTCCGTTTCTCTT CC-3′; IL-6, 5′- TCAATTCCAGAAACCGCTATGA-3′ and 5′-CACCAGCATC AGTCCCAAGA-3′; IL-1beta, 5′-CGTGCTGTCGGACCCATATGAG-3′ and 5′-GC CCAAGGCCACAGGTATTT-3′; HDAC4, 5′-AGCCTTCAGAACGGTGGTTAT-3′ and 5′-GCTGTGGATGTCCATCACTTT-3′; MEKK2, 5′-TTGTCTTTAAGCAGCC CTGAA-3′ and 5′-AAAAGTCTTCCGACCGTCATT-3′; actin, 5′-ACCCAGGCA TTGCTGACAGGATGC-3′ and 5′-CCATCTAGAAGCATTTGCGGTGGACG-3′; GAPDH, 5′-ACAACTTTGGCATTGTGGAAG-3′ and 5′-GTTGAAGTCGCAGGA GACAAC-3′.

Western Blot Analysis, Immunoprecipitation, and In Vitro Kinase Assay

Western blotting was performed as described previously (Cohen et al., 2007). For cell culture, C2C12 cells were washed with PBS twice and then lysed in extraction buffer (50 mM Tris-Cl [pH 7.4], 150 mM NaCl, 1 mM EDTA, 1% NP-40, 0.5% sodium deoxycholate, 1 mM sodium orthovanadate, 1 mM sodium fluoride, 1 mM phenylmethanesulfonylfluoride [PMSF], 0.2 mM leupeptin, protease inhibitor cocktail [Sigma]) on ice for 30 min. Lysates were cleared by centrifugation (13,000 rpm for 20 min). Protein concentrations were determined using BCA assay (Pierce). Equal amounts of cell extracts were then resolved by SDS-PAGE, transferred to nitrocellulose membranes, and probed with antibodies. Blots were detected using an ECL system (Amersham). For muscle samples, isolated TA muscles were stored in liquid nitrogen. Muscles were homogenized by glass-to-glass dounce homogenizer in suspension buffer (50 mM NaCl, 20 mM Tris [pH 7.4], 1 mM EDTA, 1 mM DTT, 1 mM sodium orthovanadate, 1 mM sodium fluoride, 1 mM PMSF, 0.2 mM leupeptin, protease inhibitor cocktail). Detergents were added to the muscle lysate (final detergent concentration; 1% NP-40, 0.5% sodium deoxycholate, 0.1% SDS) and lysates were incubated for 20 min rocking at 4°C. Lysates were cleared by centrifugation (13,000 rpm for 20 min).

For immunoprecipitation, 293T cells or C2C12 myoblasts were lysed in NETN buffer (50 mM Tris-Cl [pH 7.4], 150 mM NaCl, 1 mM EDTA, 1% NP-40, 1 mM sodium orthovanadate, 1 mM sodium fluoride, 1 mM PMSF, 0.2 mM leupeptin, protease inhibitor cocktail). Cleared supernatants by centrifugation were incubated overnight with each antibody indicated in the figure legends. For detection of MEKK2 acetylation, TA muscles were homogenized and lysed by muscle lysis condition described above and lysates were immunoprecipitated with MEKK2 antibody (Abcam). Immunoprecipitated products were analyzed by western blotting.

Kinase assay was performed as previously described (Blank et al., 1996) with slight modifications. Briefly, 293T cells were transfected with HA-MEKK2-WT or -K385Q and then lysed in NETN buffer. Whole-cell lysates were immunoprecipitated with HA-agarose beads overnight. Immunoprecipitates were washed three times with NETN buffer and twice with buffer containing 10 mM Pipes (pH 7.0), 100 mM NaCl. Beads were then incubated with purified HA-MEK1-K97M protein in kinase buffer (20 mM Pipes, 10 mM $MnCl_2$) containing 60–120 μM ATP for 30 min at 30°C. Reactions were terminated by adding 2× sample buffer and samples were analyzed for MEK phosphorylation by immunoblotting. Additionally, to purify nonacetylated and acetylated forms of MEKK2, myc-MEKK2 was cotransfected with/without HA-CBP into 293T cells. Immunoprecipitated MEKK2 with myc antibody was purified by adding myc-peptide (Sigma), according to the manufacturer's instructions. The kinase assay was performed as described above.

In Vitro Deacetylation Assay

293T cells were transfected with two sets of plasmids in 10 cm plates. One set contained pcDNA-myc-MEKK2 and pcDNA-HA-CBP. The other set contained pcDNA-Flag-HDAC4. Cells were harvested 24 hr after transfection. Cells were resuspended and incubated in 400 μl of low stringency buffer (50 mM Tris-Cl [pH 7.6], 120 mM NaCl, 0.5 mM EDTA, 0.5% NP-40) with protease inhibitors for 30 min. Lysates were cleared by centrifugation at 14K rpm for 10 min. MEKK2 and HDAC4 were pulled down by anti-myc and -Flag antibodies, respectively. After immunoprecipitation (IP) with each antibody for 3 hr, 50 μl of protein A beads (50% slurry) was added into the IP mixture and incubated for another 4 hr. Then the beads were washed three times in 1 ml Low Stringency Buffer and two times in 1 ml High Stringency Buffer (50 mM Tris-Cl [pH 7.6], 500 mM NaCl, 0.5 mM EDTA, 0.5% NP-40) and finally washed two times in 1 ml HDAC buffer (10 mM Tris-Cl [pH 8.0], 10 mM NaCl, 10% glycerol). Beads with myc-MEKK2 and Flag-HDAC4 were resuspended in 40 μl HDAC buffer, mixed together, and incubated at 37°C on rocker for 4 hr. Proteins were eluted by adding 10 μl of 4× SDS sample buffer and heating for 3 min. The supernatant was subjected to SDS-PAGE for western blot analysis. Acetylation of MEKK2 was detected by antiacetyl lysine (Ac-K) antibody.

Identification of Acetylation Sites in MEKK2

Large-scale transfection was performed in 293T cells. Myc-MEKK2 was coexpressed with HA-CBP or Flag-P/CAF and cells were lysed by the buffer used for western blot analysis. Immunoprecipitated MEKK2 with anti-myc antibody was loaded for SDS-PAGE. Following Coomassie staining/destaining (Bio-Rad), bands corresponding to MEKK2 were excised from gel.

For in-gel tryptic digestion, the gel bands were washed with 50% ethanol for 1 hr, and then again overnight. The destained gel bands were washed with deionized water twice and then were cut into small cubic pieces of about 1 mm. The gel pieces were reduced with 10 mM dithiothreitol (Sigma) at 56°C for 1 hr and then alkylated with 55 mM iodoacetamide (Sigma) at room temperature in the dark for 45 min. Enzymatic digestion was done by adding trypsin (Promega) in 50 mM ammonium bicarbonate to the gel pieces, followed by overnight incubation at 37°C and 50% acetonitrile in 5% trifluoroacetic acid (TFA) and 75% acetonitrile in 1% TFA were sequentially added to the gel pieces for the extraction of tryptic peptides. The pooled extracts were dried in a SpeedVAc, desalted with a μ-C18 ZipTip (Millipore), and then dried again prior to high-pressure liquid chromatography (HPLC)/mass spectrometry (MS)/MS analysis.

For HPLC-MS/MS analysis and database searching, peptide mixtures were analyzed by LC-MS/MS using an Eksigent NanoLC-1Dplus HPLC system (Eksigent Technologies) interfaced to an LTQ-Orbitrap Discovery instrument (ThermoFisher Scientific). The nanoliter flow LC instrument was operated with a 10 cm analytical column (75 μm inner diameter, 350 μm outer diameter) packed with Jupiter C_{12} resin (4 μm particle size, 90 Å pore size, Phenomenex). Solvent A was 0.1% formic acid in ddH_2O, and solvent B was 100% acetonitrile (Fisher Scientific) with 0.1% formic acid. Peptide samples were injected in solvent A and were separated with a gradient of 10%–90% solvent B over 40 min at a flow rate of 500 nl/min. The nanoelectrospray ion source was used with a spray voltage of 1.8 kV. No sheath, sweep, or auxiliary gasses were used, and capillary temperature was set to 180°C. The mass spectrometer was operated in a data-dependent mode to automatically switch between MS and MS/MS acquisition. Survey full-scan MS spectra (from *m/z* 350–1,500) were acquired in the Orbitrap with resolution R = 30,000 at *m/z* 400. The ten most intense ions, with singly charged precursor ions excluded, were sequentially isolated in the linear ion trap and subjected to collision induced dissociation (CID) with a normalized energy of 35%. The following MS/MS scan was used: (1) exclusion duration for the data-dependant scan: 36 s, (2) repeat count: 2, (3) exclusion window: +2 and −1 Da. The acquired data were analyzed by Mascot (v2.1, Matrix Science). Precursor mass tolerance for Mascot analysis was set at ± 2 Da, and fragment mass tolerance was set at ±0.5 Da. The database searching of all data was done with the National Center for Biotechnology Information nonredundant *Mus musculus* database. Cysteine alkylation by iodoacetamide, methione oxidation, and lysine acetylation were specified as variable modifications.

SUPPLEMENTAL INFORMATION

Supplemental Information includes seven figures and one table and can be found with this article online at doi:10.1016/j.molcel.2012.04.025.

ACKNOWLEDGMENTS

We thank Ms. A. McClure and Dr. B. Mathey-Prevot for critically reading the manuscript. We also thank Dr. Natalie G. Ahn (MKK1-wt, MKK1-8E), Eisuke Nishida (HA-c-fos), Xin Lin (myc-MEKK2), and Jennifer Y. Zhang (JNK1 DN, AP1-luc) for kindly providing constructs. This work was supported by CA126832 (NCI) to Y.Z. and AR055613 (NIAMS, NIH) to T.-P.Y. M.-C.C. was also supported in part by the National Research Foundation of Korea Grant funded by the Korean Government (NRF-2009-352-C00137).

Received: June 20, 2011
Revised: March 21, 2012
Accepted: April 20, 2012
Published online: May 31, 2012

REFERENCES

Abell, A.N., Granger, D.A., and Johnson, G.L. (2007). MEKK4 stimulation of p38 and JNK activity is negatively regulated by GSK3beta. J. Biol. Chem. *282*, 30476–30484.

Adcock, I.M. (1997). Transcription factors as activators of gene transcription: AP-1 and NF-kappa B. Monaldi Arch. Chest Dis. *52*, 178–186.

Argilés, J.M., Busquets, S., and López-Soriano, F.J. (2003). Cytokines in the pathogenesis of cancer cachexia. Curr. Opin. Clin. Nutr. Metab. Care *6*, 401–406.

Assoian, R.K. (2002). Common sense signalling. Nat. Cell Biol. *4*, E187–E188.

Bassel-Duby, R., and Olson, E.N. (2006). Signaling pathways in skeletal muscle remodeling. Annu. Rev. Biochem. *75*, 19–37.

Blank, J.L., Gerwins, P., Elliott, E.M., Sather, S., and Johnson, G.L. (1996). Molecular cloning of mitogen-activated protein/ERK kinase kinases (MEKK) 2 and 3. Regulation of sequential phosphorylation pathways involving mitogen-activated protein kinase and c-Jun kinase. J. Biol. Chem. *271*, 5361–5368.

Blonska, M., You, Y., Geleziunas, R., and Lin, X. (2004). Restoration of NF-kappaB activation by tumor necrosis factor alpha receptor complex-targeted MEKK3 in receptor-interacting protein-deficient cells. Mol. Cell. Biol. *24*, 10757–10765.

Bodine, S.C., Latres, E., Baumhueter, S., Lai, V.K., Nunez, L., Clarke, B.A., Poueymirou, W.T., Panaro, F.J., Na, E., Dharmarajan, K., et al. (2001). Identification of ubiquitin ligases required for skeletal muscle atrophy. Science *294*, 1704–1708.

Bossola, M., Pacelli, F., Tortorelli, A., Rosa, F., and Doglietto, G.B. (2008). Skeletal muscle in cancer cachexia: the ideal target of drug therapy. Curr. Cancer Drug Targets *8*, 285–298.

Bottomley, M.J., Lo Surdo, P., Di Giovine, P., Cirillo, A., Scarpelli, R., Ferrigno, F., Jones, P., Neddermann, P., De Francesco, R., Steinkühler, C., et al. (2008). Structural and functional analysis of the human HDAC4 catalytic domain reveals a regulatory structural zinc-binding domain. J. Biol. Chem. *283*, 26694–26704.

Chan, J.K., Sun, L., Yang, X.J., Zhu, G., and Wu, Z. (2003). Functional characterization of an amino-terminal region of HDAC4 that possesses MEF2 binding and transcriptional repressive activity. J. Biol. Chem. *278*, 23515–23521.

Chayama, K., Papst, P.J., Garrington, T.P., Pratt, J.C., Ishizuka, T., Webb, S., Ganiatsas, S., Zon, L.I., Sun, W., Johnson, G.L., and Gelfand, E.W. (2001). Role of MEKK2-MEK5 in the regulation of TNF-alpha gene expression and MEKK2-MKK7 in the activation of c-Jun N-terminal kinase in mast cells. Proc. Natl. Acad. Sci. USA *98*, 4599–4604.

Cohen, T.J., Waddell, D.S., Barrientos, T., Lu, Z., Feng, G., Cox, G.A., Bodine, S.C., and Yao, T.P. (2007). The histone deacetylase HDAC4 connects neural activity to muscle transcriptional reprogramming. J. Biol. Chem. *282*, 33752–33759.

Cohen, T.J., Barrientos, T., Hartman, Z.C., Garvey, S.M., Cox, G.A., and Yao, T.P. (2009). The deacetylase HDAC4 controls myocyte enhancing factor-2-dependent structural gene expression in response to neural activity. FASEB J. *23*, 99–106.

Eferl, R., and Wagner, E.F. (2003). AP-1: a double-edged sword in tumorigenesis. Nat. Rev. Cancer *3*, 859–868.

Fanger, G.R., Johnson, N.L., and Johnson, G.L. (1997). MEK kinases are regulated by EGF and selectively interact with Rac/Cdc42. EMBO J. *16*, 4961–4972.

Fischle, W., Dequiedt, F., Hendzel, M.J., Guenther, M.G., Lazar, M.A., Voelter, W., and Verdin, E. (2002). Enzymatic activity associated with class II HDACs is dependent on a multiprotein complex containing HDAC3 and SMRT/N-CoR. Mol. Cell *9*, 45–57.

Gerwins, P., Blank, J.L., and Johnson, G.L. (1997). Cloning of a novel mitogen-activated protein kinase kinase kinase, MEKK4, that selectively regulates the c-Jun amino terminal kinase pathway. J. Biol. Chem. *272*, 8288–8295.

Gomes, M.D., Lecker, S.H., Jagoe, R.T., Navon, A., and Goldberg, A.L. (2001). Atrogin-1, a muscle-specific F-box protein highly expressed during muscle atrophy. Proc. Natl. Acad. Sci. USA *98*, 14440–14445.

Guo, Z., Clydesdale, G., Cheng, J., Kim, K., Gan, L., McConkey, D.J., Ullrich, S.E., Zhuang, Y., and Su, B. (2002). Disruption of Mekk2 in mice reveals an unexpected role for MEKK2 in modulating T-cell receptor signal transduction. Mol. Cell. Biol. *22*, 5761–5768.

Haberland, M., Montgomery, R.L., and Olson, E.N. (2009). The many roles of histone deacetylases in development and physiology: implications for disease and therapy. Nat. Rev. Genet. *10*, 32–42.

Ke, H., Harris, R., Coloff, J.L., Jin, J.Y., Leshin, B., Miliani de Marval, P., Tao, S., Rathmell, J.C., Hall, R.P., and Zhang, J.Y. (2010). The c-Jun NH2-terminal kinase 2 plays a dominant role in human epidermal neoplasia. Cancer Res. *70*, 3080–3088.

Lahm, A., Paolini, C., Pallaoro, M., Nardi, M.C., Jones, P., Neddermann, P., Sambucini, S., Bottomley, M.J., Lo Surdo, P., Carfí, A., et al. (2007). Unraveling the hidden catalytic activity of vertebrate class IIa histone deacetylases. Proc. Natl. Acad. Sci. USA *104*, 17335–17340.

Macpherson, P.C., Wang, X., and Goldman, D. (2011). Myogenin regulates denervation-dependent muscle atrophy in mouse soleus muscle. J. Cell. Biochem. *112*, 2149–2159.

Mansour, S.J., Matten, W.T., Hermann, A.S., Candia, J.M., Rong, S., Fukasawa, K., Vande Woude, G.F., and Ahn, N.G. (1994). Transformation of mammalian cells by constitutively active MAP kinase kinase. Science *265*, 966–970.

McKinsey, T.A., Zhang, C.L., Lu, J., and Olson, E.N. (2000). Signal-dependent nuclear export of a histone deacetylase regulates muscle differentiation. Nature *408*, 106–111.

Molnár, A., Theodoras, A.M., Zon, L.I., and Kyriakis, J.M. (1997). Cdc42Hs, but not Rac1, inhibits serum-stimulated cell cycle progression at G1/S through a mechanism requiring p38/RK. J. Biol. Chem. *272*, 13229–13235.

Moore-Carrasco, R., García-Martínez, C., Busquets, S., Ametller, E., Barreiro, E., López-Soriano, F.J., and Argilés, J.M. (2006). The AP-1/CJUN signaling cascade is involved in muscle differentiation: implications in muscle wasting during cancer cachexia. FEBS Lett. *580*, 691–696.

Moore-Carrasco, R., Busquets, S., Almendro, V., Palanki, M., López-Soriano, F.J., and Argilés, J.M. (2007). The AP-1/NF-kappaB double inhibitor SP100030 can revert muscle wasting during experimental cancer cachexia. Int. J. Oncol. *30*, 1239–1245.

Moresi, V., Williams, A.H., Meadows, E., Flynn, J.M., Potthoff, M.J., McAnally, J., Shelton, J.M., Backs, J., Klein, W.H., Richardson, J.A., et al. (2010). Myogenin and class II HDACs control neurogenic muscle atrophy by inducing E3 ubiquitin ligases. Cell *143*, 35–45.

Morimoto, H., Kondoh, K., Nishimoto, S., Terasawa, K., and Nishida, E. (2007). Activation of a C-terminal transcriptional activation domain of ERK5 by autophosphorylation. J. Biol. Chem. *282*, 35449–35456.

Späte, U., and Schulze, P.C. (2004). Proinflammatory cytokines and skeletal muscle. Curr. Opin. Clin. Nutr. Metab. Care *7*, 265–269.

Tang, H., Macpherson, P., Marvin, M., Meadows, E., Klein, W.H., Yang, X.J., and Goldman, D. (2009). A histone deacetylase 4/myogenin positive feedback loop coordinates denervation-dependent gene induction and suppression. Mol. Biol. Cell *20*, 1120–1131.

Trosky, J.E., Li, Y., Mukherjee, S., Keitany, G., Ball, H., and Orth, K. (2007). VopA inhibits ATP binding by acetylating the catalytic loop of MAPK kinases. J. Biol. Chem. *282*, 34299–34305.

Weis, J. (1994). Jun, Fos, MyoD1, and myogenin proteins are increased in skeletal muscle fiber nuclei after denervation. Acta Neuropathol. *87*, 63–70.

Widmann, C., Gerwins, P., Johnson, N.L., Jarpe, M.B., and Johnson, G.L. (1998). MEK kinase 1, a substrate for DEVD-directed caspases, is involved in genotoxin-induced apoptosis. Mol. Cell. Biol. *18*, 2416–2429.

Yuasa, T., Ohno, S., Kehrl, J.H., and Kyriakis, J.M. (1998). Tumor necrosis factor signaling to stress-activated protein kinase (SAPK)/Jun NH2-terminal kinase (JNK) and p38. Germinal center kinase couples TRAF2 to mitogen-activated protein kinase/ERK kinase kinase 1 and SAPK while receptor interacting protein associates with a mitogen-activated protein kinase kinase kinase upstream of MKK6 and p38. J. Biol. Chem. *273*, 22681–22692.

Zhang, Y.L., and Dong, C. (2005). MAP kinases in immune responses. Cell. Mol. Immunol. *2*, 20–27.

Zhao, X., Ito, A., Kane, C.D., Liao, T.S., Bolger, T.A., Lemrow, S.M., Means, A.R., and Yao, T.P. (2001). The modular nature of histone deacetylase HDAC4 confers phosphorylation-dependent intracellular trafficking. J. Biol. Chem. *276*, 35042–35048.

Zhao, X., Sternsdorf, T., Bolger, T.A., Evans, R.M., and Yao, T.P. (2005). Regulation of MEF2 by histone deacetylase 4- and SIRT1 deacetylase-mediated lysine modifications. Mol. Cell. Biol. *25*, 8456–8464.